A Novel Image Fusion Method based on Translation Invariant Wavelet Transforms

Fen Xiao
Key Laboratory of Intelligent Computing & Information Processing of Ministry of Education, Xiangtan University, Xiangtan, China
Email: xiaof@xtu.edu.cn

Xieping Gao and Bodong Li
Information Engineering College, Xiangtan University, Xiangtan, China
Email: xpgao@xtu.edu.cn

***Abstract*—In this paper, a novel method based on translation-invariant wavelet decomposition has been introduced to the pixel level multisensor image fusion. The proposed fusion architecture is related to the "shift-decompose-fuse-shift" technique and consists of many steps. First, the source images to be shifted in both horizontal and vertical directions. The shifted images will be translated into the wavelet domain and by repeating "shift-translate" to get the decomposition of source images. Second, the different subband coefficients of the fused image are combined with the proposed fusion rule. Finally, the fused image will be obtained with the inverse translate and shift. Experimental results demonstrate that the proposed method fuses the useful information from source images and outperforms the discrete wavelet transform (DWT) and stationary wavelet transform (SWT).**

***Index Terms*—image fusion, translation-invariant wavelet, discrete wavelet transform, stationary wavelet transform**

I. INTRODUCTION

Due to the limited depth-of-field of optical lenses, it is difficult to get an image with all objects in focus. Image fusion is defined as the technique that integrates different information from several images, and creates a new image with complementary spatial and spectral resolution. Compared to the involving images, the fused image includes more comprehensive, more accurate, more stable information, more suitable for the purpose of human visual perception[1]. Image fusion is becoming one of the hottest techniques in image processing, and it has been widely used in the fields of remote sensing, medical imaging, machine vision, and military applications in recent years[2, 3].

In general, depending on the stage at which the combination mechanism takes place, image fusion can be divided into three categories, namely, pixel level, feature level and decision level[1]. Pixel level fusion means that the pixel of the fused image determined from a set of pixels in source images measured by some physical parameters[4]. Feature level fusion works on image features extracted from the source images and relies on the detection of useful features with higher confidence. Decision level fusion works at an even higher level, and merges the interpretations of different images obtained with image understanding. Both feature level and decision level fusion may involve loss of information in the information extraction process, which consequently leads to less accurate fusion results. And currently, more and more image fusion applications employ a pixel level fusion scheme.

Nowadays, there are various techniques for image fusion and most of them are belonging to pixel-level[5, 6]. A more successful method that has been explored is based on multiscale transforms. Examples include the Laplacian pyramid[4, 7], gradient pyramid[8], ratio-of-low pass pyramid[9] and discrete wavelet transform(DWT)[10-12] and stationary wavelet transform(SWT)[13]. In fact, these methods mainly focus on the pyramid decomposition of the source images. Features extracted from these coefficients can efficiently represent the characteristics of the source images. A fusion rule is then applied on these coefficients to create the multiresolution representation of the fused image. Subsequently, a fused image can be obtained by performing a reconstruction from the inverse multiresolution transform. We know that the wavelet transform is multi-scale transform and its satisfactory performance in dealing with time-frequency signal, approaches based on wavelet transform have begun to receive considerable attention[14].

However, due to the down sampling at each level, the translated image is shift-variant and this leads to the shift of image edge[15]. The results will be quickly destroyed when there is misregistration of the source images. Motivated by the better performance of translation invariant for image denoising[16, 17], we propose a pixel level image fusion based on the use of translation-invariant wavelet transformation (TIWT) in this paper. TIWT closely resembles the DWT, but uses the shifted image wavelet decomposition to get the overcomplete wavelet representation, as a result, the deterioration brings with down sampling can be avoided successfully.

On the other hand, the choice of an appropriate fusion rule is a crucial step since it defines the quality of the fusion. Many complicated fusion rules for wavelet coefficient selection have been undertaken by lots of

doi:10.4304/jsw.9.4.859-866

researchers in order to improve the quality of the fused image[5]. As the coefficients with large magnitudes correspond to salient features in the image, the simplest rule chooses-max is usually employed to multiresolution fusion scheme. Based on the fact that the HVS is primarily sensitive to local contrast changes, a rule based on activity and match measure is more appropriate since it allows to take into account the neighbourhood of the considered coefficient[4]. In this paper, a novel fusion rule based on activity measurement and advanced consistency verification has been proposed for wavelet coefficient selection to remove the shot noise.

In order to investigate the capability of the proposed scheme for image fusion, the experiments have been performed on multisensor image fusion with different multiresolution schemes (DWT, SWT and TIWT). Experiment results show that the proposed method works well for image fusion and it outperforms fusion schemes based on DWT and SWT. And the efficiency of the proposed fusion rule based on match measure followed by advanced consistency verification is also shown in the experimental result.

The rest of the paper is organized as follows. In section 2, we introduce the translation invariant wavelet transform. Section 3 proposes the fusion rule based on TIWT. Section 4 gives the detail steps and flow chart of the fusion scheme based on TIWT. The experiment results and discussion are presented in section 5. Finally, we give a conclusion in section 6.

II. Translation Invariant Wavelet Transform for Image Fusion

2.1 Translation Invariant Wavelet Transform

Let the functions $\varphi(t)(\tilde{\varphi}(t))$ and $\psi(t)(\tilde{\psi}(t))$ satisfy the required conditions for being the scaling and wavelet functions of the biorthogonal wavelet transform. And the biorthogonal wavelet system satisfies the scaling equations

$$\varphi(x)=\sqrt{2}\sum_{k\in Z}h_k\varphi(2x-k),\psi(x)=\sqrt{2}\sum_{k\in Z}g_k\psi(2x-k)$$

$$\tilde{\varphi}(x)=\sqrt{2}\sum_{k\in Z}\tilde{h}_k\tilde{\varphi}(2x-k),\tilde{\psi}(x)=\sqrt{2}\sum_{k\in Z}\tilde{g}_k\tilde{\psi}(2x-k)$$

where $\{h,g\},\{\tilde{h},\tilde{g}\}$ are lowpass and highpass filters for decomposition and reconstruction respectively. Specifically, for orthogonal wavelet, we have $\varphi(t)=\tilde{\varphi}(t)$ and $\psi(t)=\tilde{\psi}(t)$.

Using the common dilation notations $\phi_{j,k}(x)=2^{j/2}\phi(2^j x-k)$ and $\psi_{j,k}(x)=2^{j/2}\psi(2^j x-k)$, a function $f\in L^2(R)$ can be expanded into a wavelet series by

$$f=\sum_{j,k}<f,\psi_{j,k}>\tilde{\psi}_{j,k},or$$

$$f=\sum_{k}<f,\varphi_{j_0,k}>\tilde{\varphi}_{j_0,k}+\sum_{j\geq j_0,k}<f,\psi_{j,k}>\tilde{\psi}_{j_0,k}.$$

Then we have

$$c_{j-1,k}=\sum_n h_n c_{j,2k+n}, d_{j-1,k}=\sum_n g_n c_{j,2k+n} \quad (1)$$

$$c_{j,n}=\sum_k(\tilde{h}_{n-2k}c_{j-1,k}+\tilde{g}_{n-2k}d_{j-1,k}) \quad (2)$$

The discrete wavelet transform(DWT) is very efficient for computation. However the fusion results are shift-variant because of an underlying down-sampling processing. The results will be heavily deteriorated when there is mis-registration of the source images.

To overcome this problem, and motivated by the better performance of translation invariant wavelet transform in image processing[14], we decompose the source image with translation invariant wavelet transform.

Beylkin[15] proved that not all shifts are necessary and developed an efficient computational scheme for the resulting over complete wavelet representation. It is proved that, if all possible shifts of the signal f by $\tau_i\in K_D(0\leq i\leq \det(D)-1)$ are computed, where τ_i is the coset representive of the dilation matrix D, then the output of the analysis section is translation invariant. For two-dimensional image decomposition, the signal is down-sampled by 2 in the horizontal and vertical directions, i.e $D=2I_{2\times 2}$. And the corresponding shift set $K_D=\{(0,0),(0,1),(1,0),(1,1)\}$. For translation invariant wavelet transform(TIWT), one can compute the DWT for the shifted signal with $\tau_i\in K_D$ on each level, and the inverse transform technique is to make the independent inverse for each shift and then to average the separate results into one.

2.2 TIWT for Image Fusion

To simplify the description of the fusion scheme, we make an assumption that there are just two source images A and B, and the fused image is F. The schemes can be extended straightforwardly to handle more than two.

The wavelet transform is multi-scale transform and it has advantages in both space and frequency, so many multiresolution analysis based fusion schemes have appeared in literature during the last decades. A general framework for multiresolution image fusion is illustrated in Figure 1[7].

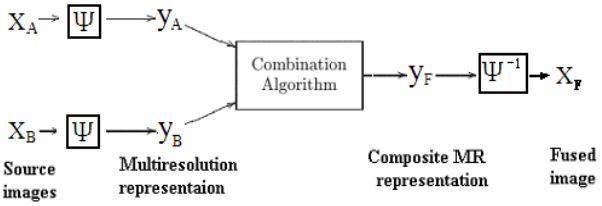

Figure 1. The general fusion scheme based on wavelet, where X and Y denote the image in spatial and transformed domains, respectively.

In short, the wavelet-based fusion method can be developed: Firstly, perform a wavelet transform on each source image X_A, X_B, resulting in a multiscale representation Y_A, Y_B of the input image. Then, a composite multiresolution representation of fused image Y_F is built by using selection schemes at different scales. This involves identifying the salient information

and transferring it into the fused image. This process, i.e., the way to combine the data, is governed by a number of rules called fusion rules. Finally, the fused image X_F is obtained by applying the inverse wavelet transform on the composite multiresolution representation.

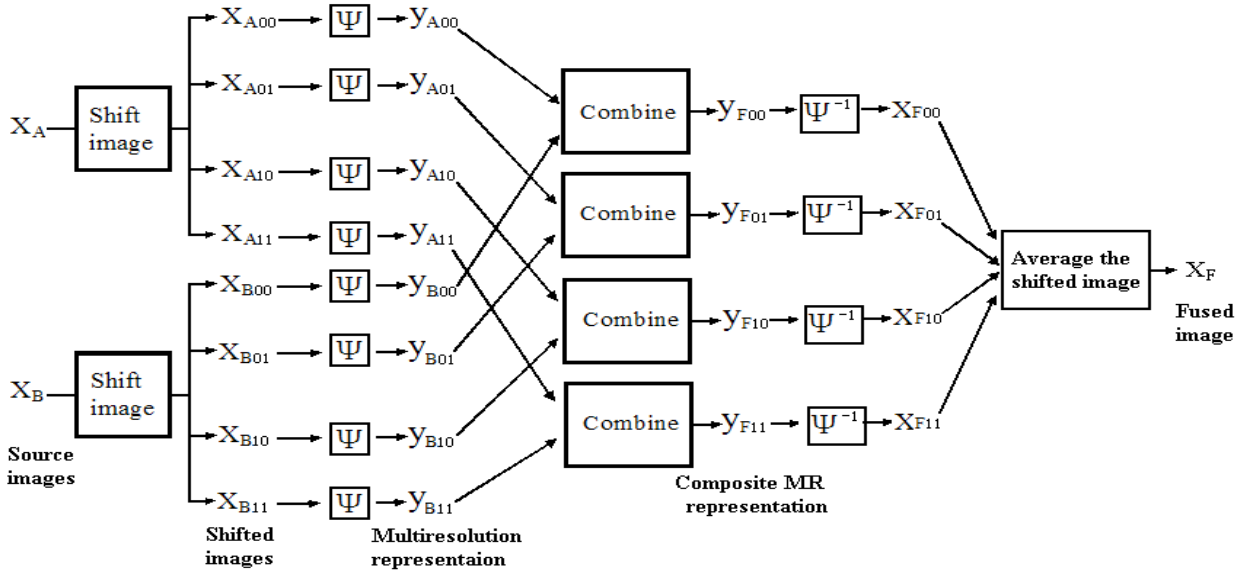

Figure 2. Translation invariant wavelet transform for image fusion scheme

For TIWT, we shifted the source images A, B and using DWT to decompose all the shifted images to get the approximation and detail sub-images. Repeating shift-decompose the approximation sub-images to get the redundancy decomposition of the source images. And the translation invariant wavelet decomposition of the fused images will obtained with the designed fusion scheme. Perform the inverse wavelet transform, finally we average over all the shifts and obtain the fused image. The basic structure of the proposed fusion scheme based on 1-level TIWT is shown in Figure 2.

III. Fusion Rules based on TIWT

The choice of an appropriate fusion rule is a crucial step since it defines the quality of the fusion. The fusion schemes especially based on multiresolution analysis have received a great attention in the literature. Because of their different physical meaning, the approximation and detail images are usually treated by the combination algorithm through different procedures.

1) The approximation image is a coarse representation of the original image and has inherited some of its properties such as the mean intensity or texture information. In our experiment, the composite approximation coefficients of the highest decomposition level, are taken to be an average of the approximation of the source:

$$F_K^0(m,n) = (A_K^0(m,n) + B_K^0(m,n))/2 \qquad (3)$$

where $F_K^0(m,n)$ is fused approximation coefficients on (m,n) at level K, A_K^0 and B_K^0 are the approximation image of the sources.

2) Detail coefficients having large absolute values correspond to sharp intensity changes and hence to salient features in the image such edges, lines and region boundaries. The simplest rule consists in taking the coefficient that has the maximum absolute amplitude. However, a rule based on a local activity measure makes them more meaningful as it takes into account the neighbourhoods.

In this section, we propose a combination algorithm that is based on an activity measure and consistency verification. The fused wavelet coefficient can be selected from the source images with the following steps: activity measure, match measure, consistency verification and weighted combination.

A. Activity Measure

An activity measure may be defined from the wavelet energy for the characterization of the dominant feature. And the local weighted energy constitutes a good indicator for activity measuring, i.e.

$$E_j^{\varepsilon}(m,n) = \sum_{m',n' \in K} w^{\varepsilon}(m',n') \left[D_j^{\varepsilon}(m+m',n+n') \right]^2 \qquad (4)$$

where $E_j^{\varepsilon}(m,n)$ is the local weighted energy of (m,n) at the level j and with orientation ε ($\varepsilon = 1,2,3$); D_j^{ε} denotes the wavelet coefficient; w^{ε} are the window's weights; K is a finite window centered at (m,n) (such as 3×3, 5×5 etc.)

B. Match Measure

This measure is supposed to quantify the similarity between the transform coefficients of the source images. We define the match value between the source images as a normalized correlation averaged over a neighbourhood of the samples:

$$M^{\varepsilon}_{j,AB}(m,n)=\frac{2\sum_{m',n'\in K} w^{\varepsilon}(m',n')D^{\varepsilon}_{j,A}(m+m',n+n')D^{\varepsilon}_{j,B}(m+m',n+n')}{E^{\varepsilon}_{j,A}(m,n)+E^{\varepsilon}_{j,B}(m,n)} \tag{5}$$

where $E^{\varepsilon}_{j,A}(m,n)$, $E^{\varepsilon}_{j,B}(m,n)$ which are obtained by (4) are the local weighted energy centered at (m,n) of the source images A, B respectively.

C. Consistency Verification

Based on the activity measure E^{ε}_{j} and the match measure $M^{\varepsilon}_{j,AB}$, we calculate the weight $\beta^{\varepsilon}_{j,A}(\cdot)$ of the decision map as [4]:

$$\beta^{\varepsilon}_{j,A}(\cdot)=\begin{cases}1 & \text{if } M^{\varepsilon}_{j,AB}(\cdot)\le T \text{ and } E^{\varepsilon}_{j,A}(\cdot)\ge E^{\varepsilon}_{j,B}(\cdot)\\ 0 & \text{if } M^{\varepsilon}_{j,AB}(\cdot)\le T \text{ and } E^{\varepsilon}_{j,A}(\cdot)< E^{\varepsilon}_{j,B}(\cdot)\\ \frac{1}{2}+\frac{1}{2}\left(\frac{1-M^{\varepsilon}_{j,AB}(\cdot)}{1-T}\right) & \text{if } M^{\varepsilon}_{j,AB}(\cdot)> T \text{ and } E^{\varepsilon}_{j,A}(\cdot)\ge E^{\varepsilon}_{j,B}(\cdot)\\ \frac{1}{2}-\frac{1}{2}\left(\frac{1-M^{\varepsilon}_{j,AB}(\cdot)}{1-T}\right) & \text{if } M^{\varepsilon}_{j,AB}(\cdot)> T \text{ and } E^{\varepsilon}_{j,A}(\cdot)< E^{\varepsilon}_{j,B}(\cdot)\end{cases} \tag{6}$$

$$\text{and } \beta^{\varepsilon}_{j,B}(\cdot)=1-\beta^{\varepsilon}_{j,A}(\cdot) \tag{7}$$

where T is the threshold for similarity comparison.

In our case, we improve the selection rule by performing consistency verification(CV) on preliminary decision weight obtained with(4)(5). Performing CV ensures that a fused coefficient does not come from a different source image from most of its neighbors and cancel the effect of noise to some extent. We calculate the local weighted decision with a 3×3 window such centered at (m,n) :

$$\beta^{\varepsilon}_{j}(m,n)=\sum_{m',n'} W'(m',n')\beta^{\varepsilon}_{j,A}(m+m',n+n'),\quad m',n'\in\{-1,0,1\} \tag{8}$$

where W' is the weighted coefficient mask. And the decision weight is defined as:

$$\beta^{\varepsilon}_{j,A}(m,n)=\begin{cases}1, & \text{if } \beta^{\varepsilon}_{j}(m,n)\ge T_1'\\ 0, & \text{if } \beta^{\varepsilon}_{j}(m,n)\le T_2'\\ \beta^{\varepsilon}_{j}(m,n), & \text{otherwise}\end{cases}$$

$$\beta^{\varepsilon}_{j,B}(m,n)=1-\beta^{\varepsilon}_{j,A}(m,n) \tag{9}$$

where thresholds T_1', T_2' satisfy: $1\ge T_1'\ge 0.5\ge T_2'\ge 0$.

D.Weigthed combination

the composite wavelet coefficients are obtained by a weighted combination:

$$D^{\varepsilon}_{j,F}(m,n)=\beta^{\varepsilon}_{j,A}(m,n)D^{\varepsilon}_{j,A}(m,n)+\beta^{\varepsilon}_{j,B}(m,n)D^{\varepsilon}_{j,B}(m,n) \tag{10}$$

where $\beta^{\varepsilon}_{j,A}(m,n), \beta^{\varepsilon}_{j,B}(m,n)$ are the weights at level j , orientation ε and position (m,n) of source images determined by the decision process.

IV.THE FUSION SCHEME BASED TIWT

It is well known that the wavelet transform and consequently the fusion results are shift-variant because of an underlying down-sampling processing. To overcome this problem, we propose a new fusion scheme based on translation invariant wavelet transform. The detailed steps of the fusion algorithm are as follows.

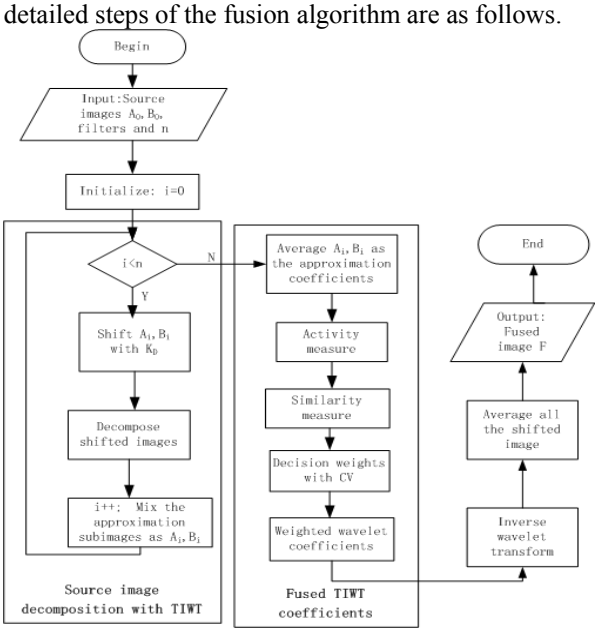

Figure 3.The flow chart of TIWT fusion scheme

Input: the source images A and B , decomposition and reconstruction filters $\{h,g,\widetilde{h},\widetilde{g}\}$, decomposition level n .

Output: the fused image F .

Step 1: Shift the source images with the shift sets $K_D=\{(0,0),(0,1),(1,0),(1,1)\}$ and obtain four image pairs A_{τ_i}, B_{τ_i} , where $\tau_i\in K_D$.

Step 2: Decompose each shifted image using Eq. (1) with the given filters h,g , the image will decompose into 4 sub-images, including one low-frequency sub-image (approximation) and three high-frequency sub-images (wavelet coefficient).

Step 3: Mix the low-frequency sub-images of the four shifts according to their origin, which will be treated as the approximation of the source image. Repeating step 1, step 2 until decompose signal with n levels and then gets a multiscale representation of the input images.

Step 4: Calculate the approximation coefficients of the fused image using Eq. (3).

Step 5: Measure the activity of the wavelet coefficient at all levels of the source image $E^{\varepsilon}_{j}(m,n)$ using Eq.(4).

Step 6: Based on $E^{\varepsilon}_{j}(m,n)$, measure the similarity of the source images on each scale $M^{\varepsilon}_{j,AB}(m,n)$ with Eq.(5).

Step 7: Based on $M^{\varepsilon}_{j,AB}(m,n)$, determining the initial weights of the wavelet coefficient using Eqs.(6)(7), and then follows consistency verification (8) to get the decision weights.

Step 8: Calculate the wavelet coefficients of the fused image of all levels using Eq.(10).

Step 9: Perform the inverse wavelet transform with (2), finally average over all the shifts and obtain the fused image F.

The implementation process of the fusion algorithm is described in detail by the above nine steps. Figure 3 shows the flowchart of the proposed fusion scheme based on TIWT.

V. EXPERIMENTS

To show the efficiency of the TI for fusing multisensor images, we compare it with the wavelet transform and stationary wavelet transform. Multifocus images and remote sensing images are used to compare the performances for each one of the wavelet decomposition and for various rules (no CV and with CV). We also demonstrate the wavelets with vanishing moment order of 4 including orthogonal ones(DB4,SA4,VM4) and biorthogonal ones(CDF44 and DD44) for fusion, which are widely used in image processing. Our experiments were performed on a 3.3 GHz Pentium Dual-Core CPU, 2.0GB of main memory and Matlab 7.0.

5.1 Dataset

In order to investigate the fusion performance of the proposed image fusion scheme described in previous section, we perform image fusion on the multifocus images and remote sensing images. For multifocus images fusion, three commonly used image samples were tested: balloon (of size 480×640), Field (512×512) and lab (480×640). For balloon, the reference image with good focus everywhere shown in Fig.3(a). The simulated multi-focus images in Fig.3(b) and Fig.3(c) were generated by performing Gaussian blurring (radius=2.0) on the left and right, respectively. Two pairs of multifocus images including clock and lab (shown in Fig.4 and Fig.5) are also used for evaluation, both of them have no reference image. For remote sensing fusion, we selected a pair of registered 512×512 infrared image and visible light image (Fig.6).

5.2 Experimental Setting

In this paper, three wavelet-based decomposition algorithms with different selection rule have been employed, which are conventional discrete wavelet transforms, stationary wavelet transform and translation invariant wavelet transform. In order to compare the performance of different wavelet, a series wavelet including orthogonal wavelet, biorthogonal wavelet, multiwavelet and nonseparable wavelet have been used in our experiment. For all wavelet transform, we use five levels of decomposition. The coefficients of three orientations ε ($\varepsilon=1,2,3$) be treated in the same way and a 3×3 window with the weights

$$w^{\varepsilon}=W'=\begin{bmatrix}1/16 & 1/8 & 1/16\\ 1/8 & 1/4 & 1/8\\ 1/16 & 1/8 & 1/16\end{bmatrix}$$

are used for activity measurement and consistency verification in our case. The thresholds for decision map T, T_1', T_2' are 0.5, 0.75 and 0.25 respectively.

5.3 Quantitative Evaluation of the Fused Method

Three criteria are employed to evaluate the performance of each image fusion algorithm, which are the root mean squared error, mutual information and entropy.

The RMSE is the natural measure of image quality if there is a "ground truth" image available. For reference image R and fused image F, $RMSE$ can be defined as:

$$RMSE=\sqrt{\frac{1}{M\times N}\sum_{i=1}^{M}\sum_{j=1}^{N}(R(i,j)-F(i,j))^2} \tag{11}$$

where $R(i,j)$ and $F(i,j)$ are the image pixel values of the reference image and the fused image respectively, $M\times N$ is the image size. The RMSE is used to measure the difference between the reference image and the fused image. The less the value is, the better fusion results we get.

We give the definition of mutual information as:

$$MI=\sum_{i=0}^{L-1}\sum_{j=0}^{L-1}h_{R,F}(i,j)\log_2\frac{h_{R,F}(i,j)}{h_R(i)h_F(j)} \tag{12}$$

where $h_{R,F}$ is the normalized joint grey level histogram of images R and F, h_R and h_F are the normalized marginal histograms of the two images, L is the number of grey levels. Mutual information indicates how much information the fused image conveys about the reference, and so a larger MI is preferred.

It should be noticed that the first two criteria is based on the presence of the reference image. Unfortunately, in general, there are no ground truths for realistic image fusion problems. We employ information entropy as the third criterion, defined as:

$$H=-\sum_{i=0}^{L-1}h_F(i)\log_2(h_F(i)) \tag{13}$$

The information entropy measures the richness of information in an image. The bigger the entropy H is, the better performance of the fused image.

5.4 Results and Discussion

In this section, we present and discuss the experimental results. Tables 1-3 give the performance parameters(RMSE, MI and Entropy) value of fusion schemes on balloon images. As can be seen from tables1-3, values of the entropy are quite consistent with currently used metrics such as RMSE or MI, which provides a good indication of the actual performance of fusion schemes. So in the following analysis, all comparisons were focused on the Entropy metric. We list the Entropy value of image fusion schemes on processing the remaining image pairs in Tables 4-6. Because of the

lack of space, fusion images are reported only for the DB4 TIWT with consistency verification.

As can be seen from the tables, several observations can be made:

1). Translation invariant wavelet transform shows marked improvements over the others, the performance of the stationary wavelet transform better than the convention discrete wavelet transform.

2). The proposed fusion rule based on activity match measurement together with a window-based consistency verification adds robustness to the fusion system as it provides a smoother activity function. It improves noticeably the quality of the fusion compared to state-of-art fusion rules and constitutes a more appropriate rule for fusing multisensor image.

3). From the quantitative results, we can conclude that the fusion result obtained by the biorthogonal wavelet filters is generally better than the result generated by orthogonal one.

IV. Conclusion

In this paper, a novel fusion method has been proposed for performing the pixel level fusion of spatially registered image. This fusion method is based on a translation invariant extension of discrete wavelet transform which yields an overcomplete signal representation. In order to make good use of the redundant wavelet coefficient, we further introduced an efficient fusion rule based on activity match measure and advanced consistency verification. Experimental results show that the translation invariant wavelet decomposition turns out to be preferable to the standard wavelet approaches whatever the selected fusion rule. The particularity of the redundant information lies in performing wavelet transform on shifted image, which allows flexibility for defining the fusion rule. This property allows ensuring a better detection of significant features. From these considerations, we can conclude that the translation invariant wavelet decomposition constitutes a more robust approach for image fusion than the stationary wavelet transform and wavelet decomposition. The more efficient fusion rule based on translation invariant wavelet representation needs to be investigated in the future.

Acknowledgment

The work was partly supported by the National Natural Science Foundation of China(Grant Nos. 61202192, 61172171) and the Specialized Research Fund for the Doctoral Program of Higher Education(Grant No. 20104301120002)

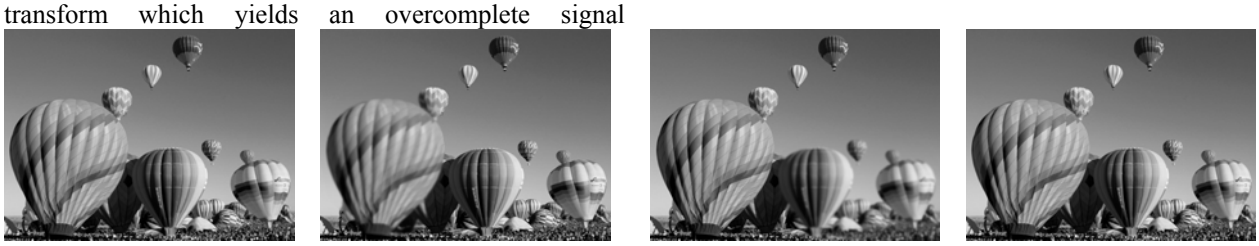

(a) (b) (c) (d)

Figure 4. The “Balloon” reference image, blurred image and fused image. (a) Reference image (all in focus); (b) focus on the right, blurring the left part; (c) focus on the left, blurring the right part; (d) fused image by TIWT

(a) (b) (c)

Figure 5. The “Field” source images and fused image, (a) source image 1; (b) source image 2; (c) fused image by TIWT

(a) (b) (c)

Figure 6. The “Lab” source images and fused image, (a) Focus on the clock; (b) focus on the student; (c) fused image by TIWT

(a) (b) (c)

Figure 7. Image fusion with remote sensing images, (a) infrared image; (b)Visible light image (c) fused image by TIWT

TABLE 1.
RMSES OBTAINED BY DIFFERENT FUSION METHODS ON PROCESSING BALLOON

	DWT		SWT		TIWT	
	No CV	CV	No CV	CV	No CV	CV
DB4	0.6938	0.6938	0.6852	0.6167	0.4276	**0.3365**
SA4	0.8666	0.7289	0.6823	0.6289	0.4872	**0.4283**
VM4	0.5511	0.4823	0.5493	0.5018	0.4780	**0.4272**
CDF44	0.6678	0.6678	0.6426	0.5852	0.3472	**0.2553**
DD44	0.7120	0.7120	0.6545	0.5946	0.3769	**0.2830**

TABLE 2.
MIS OBTAINED BY DIFFERENT FUSION METHODS ON PROCESSING BALLOON

	DWT		SWT		TIWT	
	No CV	CV	NCV	CV	No CV	CV
DB4	4.5508	4.6105	4.4512	4.5233	4.7817	**4.8353**
SA4	4.4653	4.5216	4.5974	4.6351	4.7231	**4.7504**
VM4	4.6198	4.6731	4.5894	4.6425	4.7240	**4.7637**
CDF44	4.5466	4.5803	4.4912	4.5479	4.8938	**4.9418**
DD44	4.5352	4.5592	4.4664	4.5216	4.8696	**4.8852**

TABLE 3.
ENTROPIES OBTAINED BY DIFFERENT FUSION METHODS ON PROCESSING BALLOON

	DWT		SWT		TIWT	
	No CV	CV	NCV	CV	No CV	CV
DB4	7.2792	7.3447	7.3104	7.3333	7.3912	**7.4297**
SA4	7.1810	7.2686	7.2634	7.3095	7.2856	**7.3334**
VM4	7.2627	7.3513	7.3475	7.3705	7.3230	**7.3946**
CDF44	7.2999	7.3132	7.3068	7.3278	7.3984	**7.4167**
DD44	7.2976	7.3106	7.2859	7.3125	7.4033	**7.4198**

TABLE 4.
ENTROPIES OBTAINED BY DIFFERENT FUSION METHODS ON PROCESSING FIELD

	DWT		SWT		TIWT	
	No CV	CV	NCV	CV	No CV	CV
DB4	4.9848	4.9909	5.1306	5.1148	5.1337	**5.1339**
SA4	5.0467	5.0194	5.0316	5.0191	5.0863	**5.0989**
VM4	4.9875	5.0096	5.0746	**5.0882**	5.0411	5.0738
CDF44	5.0250	5.0399	5.1167	5.1066	**5.1233**	5.1030
DD44	5.0156	5.0401	5.0927	5.0710	5.1502	**5.1533**

TABLE 5.
ENTROPIES OBTAINED BY DIFFERENT FUSION METHODS ON PROCESSING LAB

	DWT		SWT		TIWT	
	No CV	CV	NCV	CV	No CV	CV
DB4	6.8775	6.8403	6.9070	6.9019	7.0104	**7.0153**
SA4	6.8841	6.8903	6.8954	6.9063	6.9118	**6.9434**
VM4	6.8014	6.8474	6.8432	6.8581	6.8748	**6.8880**
CDF44	6.8863	6.9045	6.8752	6.8856	7.0327	**7.0527**
DD44	6.8885	6.8969	6.8609	6.8818	7.0333	**7.0398**

TABLE 6.
ENTROPIES OBTAINED BY DIFFERENT FUSION METHODS ON PROCESSING REMOTE SENSING IMAGE

	DWT		SWT		TIWT	
	No CV	CV	No CV	CV	No CV	CV
DB4	7.0253	7.0612	7.0437	7.0870	7.0696	**7.0877**
SA4	6.9624	7.0374	7.1311	**7.1604**	7.0411	7.0816
VM4	6.8356	6.8469	7.0935	**7.1264**	7.0681	7.0905
CDF44	6.9680	7.0162	**7.1144**	7.1050	7.0972	7.1067
DD44	6.9449	7.0081	7.1143	**7.1273**	7.1159	7.1146

REFERENCES

[1] P. K. Varshney, "Multisensor data fusion," *Electronics & Communication Engineering Journal*, vol. 9, pp. 245-253, 1997.

[2] X. Gong, J. Zhou, H. Wu, G. Lei, and X. Li, "Application to Three-Dimensional Canonical Correlation Analysis for

Feature Fusion in Image Recognition," *Journal of Computers*, vol. 6, pp. 2427-2433, 2011.
[3] S. Fang, R. Deng, Y. Cao, and C. Fang, "Effective Single Underwater Image Enhancement by Fusion," *Journal of Computers*, vol. 8, pp. 904-911, 2013.
[4] P. J. Burt and R. J. Kolczynski, "Enhanced image capture through fusion," presented at Proceeding of the 4th International Conference on Computer Vision, Berlin,Germany, 1993.
[5] G. Piella, "A general framework for multiresolution image fusion: from pixels to regions," *Information Fusion*, vol. 4, pp. 259, 2003.
[6] X. Cai, G. Han, and J. Wang, "Image Fusion Method Based on Directional Contrast-Inspired Unit-Linking Pulse Coupled Neural Networks in Contourlet Domain," *Journal of Computers*, vol. 8, pp. 1544-1551, 2013.
[7] P. J. Burt and E. H. Adelson, "The Laplacian pyramid as a compact image code," *IEEE. Trans. on Communications*, vol. 31, pp. 532-540, 1983.
[8] V. S. Petrovic and C. S. Xydeas, "Gradient-Based Multiresolution Image Fusion," *IEEE Transactions on Image Processing*, vol. 13, pp. 228-237, 2004.
[9] A. Toet, L. V. Ruyven, and J. Valeton, "Merging thermal and visual images by a contrast pyramid," *Optical Engineering*, vol. 28, pp. 789-792, 1989.
[10] G. Pajares and J. Manuel de la Cruz, "A wavelet-based image fusion tutorial," *Pattern Recognition*, vol. 37, pp. 1855-1872, 2004.
[11] H. Li, M. B. S., and M. S. K., "Multisensor Image Fusion Using the Wavelet Transform," *Graphical Models and Image Processing*, vol. 57, pp. 235, 1995.
[12] L. Shutao and Y. Bin, "Multifocus image fusion by combining curvelet and wavelet transform," *Pattern Recognition Letters*, vol. 29, pp. 1295-1301, 2008.
[13] Y. Chai, H. F. Li, and M. Y. Guo, "Multifocus image fusion scheme based on features of multiscale products and PCNN in lifting stationary wavelet domain," *Optics Communications*, vol. 284, pp. 1146-1158, 2011.
[14] Z. Yufeng, E. E. A., H. B. C., and H. A. M., "A new metric based on extended spatial frequency and its application to DWT based fusion algorithms," *Information Fusion*, vol. 8, pp. 177, 2007.
[15] S. Mallat, "A theory for multiresolution signal decomposition: the wavelet representation," *IEEE Transactions on Pattern Analysis and Machine Intelligence*, vol. 11, pp. 674-693, 1989.
[16] T. D. Bui and C. Guangyi, "Translation-invariant denoising using multiwavelets," *IEEE Transactions on Signal Processing*, vol. 46, pp. 3414-3420, 1998.
[17] G. Liu, J. Liu, Q. Wang, and W. He, "The Translation Invariant Wavelet-based Contourlet Transform for Image Denoising," *Journal of Multimedia*, vol. 7, pp. 254-261, 2012.

Fen Xiao was born in 1981. She received the B.S. degree in computer science and the Ph.D. degree in computational mathematics from Xiangtan University, China, in 2002 and 2008, respectively.

She is currently an Associate Professor and a tutor for graduate in the College of Information Engineering of Xiangtan University. She is a regular reviewer for several journals and some kinds of projects. She has authored and co-authored over 10 journal papers and conference papers, such as IEEE Transactions on image processing, Software Journal. Her research interests focus on image processing, wavelet analysis theory and neural network.

Fen Xiao is the member of the China Computer Federation. And she received the Excellent Doctoral Dissertation Awards of the Hunan Province, China.

Xieping Gao was born in 1965. He received the B.S.and M.S. degrees from Xiangtan University of China in 1985 and 1988, respectively. He received the Ph.D. degree from Hunan University, China, in 2003.

He is a Professor with the College of Information Engineering at Xiangtan University, China. He was a visiting scholar at the National Key Laboratory of Intelligent Technology and Systems, Tsinghua University, China, from1995 to 1996 and at the School of Electrical & Electronic Engineering, Nanyang Technological University, Singapore, from 2002 to 2003. He is a regular reviewer for several journals and he has been a member of the technical committees of several scientific conferences. He has authored and co-authored over 80 journal papers, conference papers and book chapters. His current research interests are in the areas of wavelets analysis, neural networks, evolution computation and image processing.

Bodong Li was born in 1980. He received the B.S. degree in computer science and the Ph.D. degree in computational mathematics from Xiangtan University, China, in 2004 and 20010, respectively.

Now, he is an Associate Professor in the College of Information Engineering of Xiangtan University. He has authored and co-authored over 10 journal papers and conference papers. His recent research interests include wavelet analysis and signal processing.